Published in Molecular and Cellular Neurosciences 25: 650-663, 2004

Parvalbumin deficiency affects network properties resulting in increased susceptibility to epileptic seizures

B. Schwaller,[a,*] I.V. Tetko,[b] P. Tandon,[c] D.C. Silveira,[c] M. Vreugdenhil,[d] T. Henzi,[a] M.-C. Potier,[e] M.R. Celio,[a] and A.E.P. Villa[b,f]

[a] *Division of Histology, Department of Medicine, University of Fribourg, CH-1700 Fribourg, Switzerland*
[b] *Laboratoire de Neuroheuristique, Institute of Physiology, University of Lausanne, Lausanne, Switzerland*
[c] *Department of Neurology, Children's Hospital and Harvard Medical School, Harvard Institute of Medicine, Boston, USA*
[d] *Division of Neuroscience, Department of Neurophysiology, Medical School, University of Birmingham, Edgbaston, Birmingham, UK*
[e] *Laboratoire de Neurobiologie, CNRS UMR7637, ESPCI, Paris, France*
[f] *Laboratoire de Neurobiophysique, INSERM U318, Université "Joseph Fourier", Grenoble 1, France*

Received 6 August 2003; revised 1 December 2003; accepted 9 December 2003

Networks of GABAergic interneurons are of utmost importance in generating and promoting synchronous activity and are involved in producing coherent oscillations. These neurons are characterized by their fast-spiking rate and by the expression of the Ca^{2+}-binding protein parvalbumin (PV). Alteration of their inhibitory activity has been proposed as a major mechanism leading to epileptic seizures and thus the role of PV in maintaining the stability of neuronal networks was assessed in knockout (PV−/−) mice. Pentylenetetrazole induced generalized tonic–clonic seizures in all genotypes, but the severity of seizures was significantly greater in PV−/− than in PV+/+ animals. Extracellular single-unit activity recorded from over 1000 neurons in vivo in the temporal cortex revealed an increase of units firing regularly and a decrease of cells firing in bursts. In the hippocampus, PV deficiency facilitated the $GABA_A$ergic current reversal induced by high-frequency stimulation, a mechanism implied in the generation of epileptic activity. We postulate that PV plays a key role in the regulation of local inhibitory effects exerted by GABAergic interneurons on pyramidal neurons. Through an increase in inhibition, the absence of PV facilitates synchronous activity in the cortex and facilitates hypersynchrony through the depolarizing action of GABA in the hippocampus.

Introduction

A finely tuned balance between excitatory and inhibitory activity in a neuronal circuit is required for appropriate brain function. Anatomical and/or chemical alterations resulting from changes in excitatory (glutamatergic) or inhibitory (GABAergic) activity can lead to sustained, abnormally synchronous and excessive discharges of large populations of neurons, which is manifested as epileptic seizures (Aird and Gordon, 1993; Bernard et al., 1999; Engel, 1996; Prince, 1999). In the cerebral cortex, γ-aminobutyric acid (GABA)-containing interneurones control pyramidal cell activity, restrict excitation both in a feedback and feedforward manner (Chagnac-Amitai and Connors, 1989; Kisvarday et al., 1994), and are critical to synchronous activity (Jones, 1993; Lytton and Sejnowski, 1991; Somogyi et al., 1998). The subpopulation of inhibitory, GABAergic interneurones expressing the EF-hand calcium-binding proteins parvalbumin (PV) or calbindin D-28k (CB), and in particular PV-expressing chandelier cells play an important role in controlling pyramidal cell excitability (Marco et al., 1996; for review, see DeFelipe, 1997). These neurons are also thought to be important in the regulation and control of seizure activity (Mihaly et al., 1997). PV is a cytosolic low-molecular weight (M_r 12 kDa), high-affinity Ca^{2+}-binding protein and the intracellular concentration in interneurones was reported to be in the order of 50 μM (Plogmann and Celio, 1993). It has been proposed that efficient Ca^{2+} buffering by PV and its high concentration in PV-expressing nonpyramidal cells is a prerequisite for the proficient inhibition of cortical networks (DeFelipe, 1997). To investigate this hypothesis, we used mice lacking PV (PV−/−), which had previously been produced by homologous recombination (Schwaller et al., 1999). These mice show no obvious abnormalities when maintained under standard housing conditions and the frequency of homozygous animals is approximately 25%, indicating that embryonic development is not altered in these animals. In PV−/− mice, changes in the contraction/relaxation cycle of fast-twitch muscles, which in WT animals contain significant amounts of PV, can be directly correlated with the absence of this slow-onset Ca^{2+} buffer. The amplitude of a Ca^{2+} transient after a brief electrical stimulation is not changed, but the initial decay of $[Ca^{2+}]_i$ is significantly reduced in the absence of PV (Schwaller et al., 1999). A similar effect of PV on the kinetics of Ca^{2+} transients is detected in PV-injected chromaffin cells (Lee et al., 2000b) and more important in a subpopulation of inhibitory hippocampal neurons (Lee et al., 2000a). In terms of the specific function of PV, the kinetics of Ca^{2+}-binding and-release is likely to be important. We have demonstrated that the

* Corresponding author. Division of Histology, Department of Medicine, University of Fribourg, 14, Chemin du Musee, CH-1700 Fribourg, Switzerland. Fax: +41-26-300-97-32.
E-mail address: Beat.Schwaller@unifr.ch (B. Schwaller).

1044-7431
doi:10.1016/j.mcn.2003.12.006

lack of PV presynaptically in the axo-axonic (chandelier) and basket cells of the cerebellum affects the paired-pulse modulation at this synapse to the Purkinje cell (Caillard et al., 2000). In WT mice, this synapse shows paired-pulse depression, which changes to paired-pulse facilitation in PV−/− mice at short time intervals (<100 ms). In the hippocampus, PV deficiency facilitated repetitive IPSCs at frequencies >20 Hz and the power of related inhibition-based gamma oscillations was increased (Vreugdenhil et al., 2003). Thus, PV is able to affect short-term modulation that likely affects temporal aspects of the entire network containing PV-expressing neurons. In this report, we investigated the effects of PV deficiency on the stability of cortical neuronal networks. We challenged the networks in vivo using the convulsant drug pentylenetetrazole, assessed the firing properties of pyramidal cells in the temporal neocortex in vivo, and assessed the consequence of facilitation of GABA release with high-frequency activity in hippocampal slices.

Results

Distribution of PV-immunoreactive (PV-ir) neurons and neurons containing similar abundantly expressed Ca^{2+}-binding proteins in the brain of PV−/− mice are not altered

The genotype of each mouse was determined by PCR as described before (Schwaller et al., 1999). The distribution and

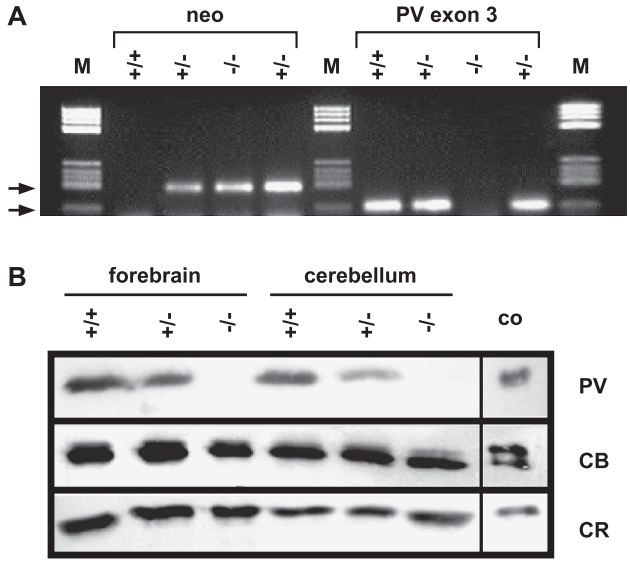

Fig. 1. (A) Genotyping of PV-KO mice by PCR. Amplification of either PV exon 3 (151 bp, lower arrow) or part of the neocassette (188 bp, upper arrow) allows for the distinction between the WT (+) or mutated allele (−). Genotypes of the four mice analyzed are indicated. As marker (M), Std. V from Roche was used. (B) Western blot of soluble proteins extracted from forebrain and cerebellum of PV+/+, PV+/−, or PV−/− mice using antibodies specific for parvalbumin (PV), calbindin D-28k (CB), or calretinin (CR). Total protein loads of forebrain and cerebellum proteins on gels were adapted to obtain similar staining intensities on Western blots: PV (60 and 10 μg), CB (20 and 5 μg), and CR (20 and 10 μg), respectively. Purified recombinant proteins (PV: 25 ng; CB: 40 ng; CR: 25 ng) were used as controls (co). On all three membranes, one single protein of the correct size was recognized by each of the three antibodies and only the regions of interest are shown.

Table 1
Parvalbumin ELISA: values[a] in μg/mg of soluble protein

	Forebrain	Cerebellum	Kidney	TA	EDL
PV+/+	1.53	9.8	1.81	37.5	27.6
PV+/−	0.52	2.95	0.57	19.46	9
PV−/−	∅	∅	∅	∅	∅
% PV in PV+/− vs. PV+/+	34[a]	30	31	52	33

TA = tibialis anterior; EDL = extensor digitorum longus; ∅ = not detectable; [PV] < 25 ng/mg protein).
[a] Mean of two animals per genotype.

expression levels of PV were investigated in the three genotypes. Western blot analysis of cytosolic proteins extracted from forebrain or cerebellum revealed the complete absence of a positive signal in PV−/− mice and reduced signal in PV+/− animals compared to the WT ones (Fig. 1). A sandwich ELISA method was used to quantify the amounts of PV present in the different genotypes. In both the cerebellum and the forebrain, the PV content in the heterozygous mice was reduced to 30–40% compared to WT mice (Table 1). In this genotype (PV+/−), PV levels in some other organs with significant expression of PV (kidney, fast-twitch muscles tibialis anterior and extensor digitorum longus) were analyzed and also found to be approximately 30–50% compared to WT mice (Table 1). PV-expressing cells are characterized by the presence of "perineuronal nets", a specific extracellular matrix (ECM) containing chondroitin sulphate proteoglycans (e.g., neurocan and phosphacan), which can be visualized by the staining of *N*-acetylgalactosamine specific lectins (Celio et al., 1998; Kosaka and Heizmann, 1989). Binding sites for *Vicia villosa* agglutinin (VVA), *Wisteria floribunda* agglutinin (WFA) or soybean agglutinin (SBA) are present at high densities on the surface of PV-expressing nonpyramidal cells. The developmental expression of PV is in temporal association with the beginning of physiological activity (Solbach and Celio, 1991; Soriano et al., 1992). Thus, the question is raised whether the lack of PV in the knockout animals leads to the absence or degeneration of this subpopulation of nonpyramidal cells expressing PV in WT animals. It is also possible that other cell types in the knockout animals replaced the cells originally expressing PV in the WT ones. Our results indicate that the three genotypes (PV+/+, PV+/−, and PV−/−) show no apparent alterations in distribution or the number of interneurons throughout the cerebral cortex (Fig. 2A) and the multipolar interneurones of the hippocampus (Vreugdenhil et al., 2003; data not shown) in VVA-stained brain sections. A detailed immunofluorescence analysis by laser scanning confocal microscopy on WFA-stained perineuronal nets around cortical interneurones of PV−/− mice revealed no differences compared to WT mice (Haunso et al., 2000). PV-expressing cells not only share a specific staining, they can also be recognized by specific discharge properties. In the rat cortex, PV-expressing nonpyramidal cells are characterized as fast-spiking (FS) cells and spike trains elicited by depolarizing current pulses in FS cells show almost no spike-frequency adaptation (Kawaguchi and Kubota, 1993, 1997). Preliminary results from similar experiments performed on PV−/− mice showed that FS cells with discharge properties identical to WT mice can be identified (M. Galarreta and S. Hestrin, personal communications). Both anatomical and electrophysiological results suggest that the inhibitory interneurones normally expressing PV (including the chandelier and basket cells) were not eliminated or replaced by another subpopulation of nerve cells and are still present in the cortex of PV-deficient mice.

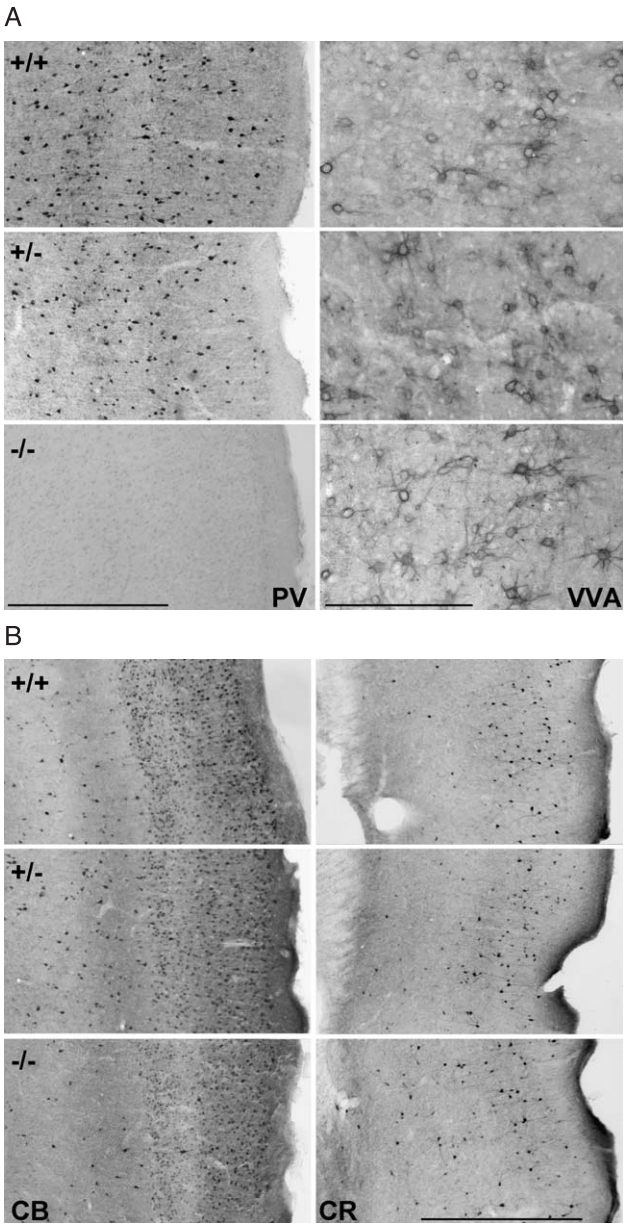

Fig. 2. Immunohistochemistry of 40-μm cryostat brain sections (temporal cortex) from the three genotypes stained with antisera against PV, CB, and CR. Perineuronal nets around PV-expressing neurons were stained with peroxidase-coupled isolectin B4 *V. villosa* agglutinin (VVA). Scale bar for PV, CB, and CR images: 500 μm; for VVA: 200 μm. (A) PV and VVA staining; (B) CB and CR. Due to the thickness of the sections, not all immunostained neurons are in the same focal plane.

Since in a small population (≈5%) of GABAergic interneurones, the Ca^{2+}-binding proteins PV and CB are coexpressed, we investigated whether the number of CB-expressing cells was up-regulated in PV−/− mice. The expression pattern of the closely related protein calretinin (CR) was also analyzed. In all three genotypes, the expression patterns of CB- and CR-immunoreactive cells in the neocortex was qualitatively not different (Fig. 2B). This was the case for the distribution in the different cortical layers as well as the density of CB- and CR-ir neurons. Western blot analysis of cytosolic proteins isolated from forebrain and cerebellum of PV−/− mice also failed to show any up-regulation of CR or CB (Fig. 1) and also no changes in mRNA levels of CB and CR were observed with microarray analysis (not shown). We cannot discard the possibility that levels of CB in individual neurons expressing both, CB and PV (e.g., Purkinje cells in the cerebellum) are higher than in WT animals to compensate for the lack of PV. In the neocortex and hippocampus, where functional experiments were carried out in vivo and in vitro (see below), the coexpression of any two of these proteins is a very rare event.

The relative abundance of GABA(R) mRNAs and selected GABA(R) protein is not changed in PV−/− mice

The lack of PV in presynaptic terminals has been show to affect GABAergic transmission as evidenced by altered paired-pulse modulation at the synapse between stellate/basket cells and Purkinje cells (Caillard et al., 2000) and by increased facilitation of repetitive IPSCs in the hippocampus (Vreugdenhil et al., 2003). Thus, we hypothesized that PV deficiency could induce compensation mechanisms such as changes in the amount, distribution, or subunit composition of different GABA receptors. At the global level, differential expression analysis between PV+/+ and PV−/− cerebellum and forebrain using cDNA microarrays containing 96 genes involved in neurotransmission including 13 subtypes of GABA receptors revealed no significant changes except for PV transcripts. At the protein level, semiquantitative Western blot analysis of the $GABA_A$ receptor subunits α2, α3, and β2/3 showed no significant differences between PV−/− and PV+/+ mice (Fig. 3).

PV−/− mice manifest a higher sensitivity toward the convulsant drug pentylenetetrazole (PTZ)

Epilepsy, one of the most common neurological disorders, is characterized by massive hypersynchronous discharges from large assemblies of neurons (Traub et al., 1996). Previous findings on altered short-term plasticity and increased power at gamma frequency in PV−/− brain in vitro (Caillard et al., 2000; Vreugdenhil et al., 2003) led us to hypothesize that subtle changes in the temporal aspects of network signaling could thus affect the susceptibility to epileptic seizures. We have used pentylenetetrazole (PTZ) to induce acute epileptic seizures (Loscher and Nolting, 1991; Olsen, 1981; Stone and Javid, 1979; Yonekawa et al., 1980). Animals were injected with PTZ (50–70 mg/kg, i.p.) and the seizure intensity as well as the time until onset of clonic–tonic seizures (CTS) was measured. At the lowest dose tested (50 mg/kg), the average seizure stage was not significantly different in the three genotypes [6.0 ± 0.7, 6.0 ± 0.6, and 6.1 ± 0.2 for PV−/− (n = 6), PV+/−(n = 6), and PV+/+ (n = 12), respectively]. At a

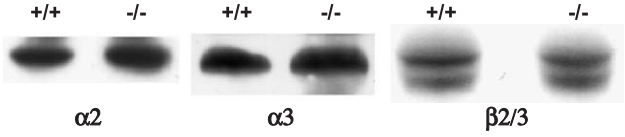

Fig. 3. Relative levels of $GABA_A$(R) subunits in the forebrain determined by Western blot analysis. Representative Western blot signals for the GABA receptor subunits α2, α3, and β2/β3 in PV+/+ and PV−/− mice. Semiquantitative analysis of ECL signals (n = 3 animals for both genotypes) revealed no significant differences between PV+/+ and PV−/− samples.

dose of 60 mg/kg PTZ (Fig. 4A), the majority of animals (approximately 90%, irrespective of the genotype) showed generalized clonic–tonic seizures, characterized by forelimb and/or hindlimb clonus and tonus resulting in episodes of falling down (seizure stage ≥ 6). While also at 60 mg/kg, PTZ-induced seizures in PV+/+ and PV+/− mice were classified as stage 6, PV−/− mice in the average were classified as stage 7. Fig. 4B shows the relative distribution of seizure stages 5–8 reached by the three genotypes at 60 mg/kg PTZ. A significant shift toward increased seizure intensity is evident from PV+/+ to PV−/− mice. The percentage of animals reaching status epilepticus (SE, seizure stage ≥ 7) was significantly higher in PV−/− mice (78% vs. 16% for WT and PV+/− animals, respectively; Fig. 4B). The severity of SE was so intense that 34% of the PV−/− mice and 5% of the PV+/− animals died after the PTZ administration (seizure stage 8), while all PV+/+ animals survived (Fig. 4B). At the highest dose tested (70 mg/kg PTZ), most animals went into SE leading to death of 66% of PV−/− mice compared to 33% in both PV+/− and WT animals (Fig. 4A). Thus, also at this dose, the severity of PTZ-induced epileptic seizures was higher in PV−/− mice compared to the other two groups. As in the electrophysiological recordings, the question of the genetic background was also addressed in the PTZ experiments. For this purpose, a F1 generation between 129/SvEv and C57BL/6J mice were bred and compared with the PV+/+ mice. The susceptibility of these mice to 60 mg/kg of PTZ was not significantly different from the PV+/+ (129P2 × B6) mice [seizure stage: 6.00 ± 0.14 for PV+/+ (n = 18) vs. 6.00 ± 0.19 for F1 129/SvEv × C57BL/6J mice (n = 16)].

The onset of seizure activity due to PTZ depends mainly on two parameters: the threshold concentration of PTZ to cause epileptic seizures needs to be reached and a ‘critical’ mass of neurons needs to be affected. As the concentration of PTZ is increased from 50 to 70 mg/kg, the time of onset of CTS decreased from approximately 300 to 90 s in all three genotypes (Fig. 4C). This most likely reflects the kinetics of uptake into the vascular system and thus the critical concentration to induce seizures is reached earlier when higher concentrations of PTZ are used. Of note, the latency of CTS onset was consistently slightly longer in PV−/− mice at all three doses of PTZ tested (Fig. 4C).

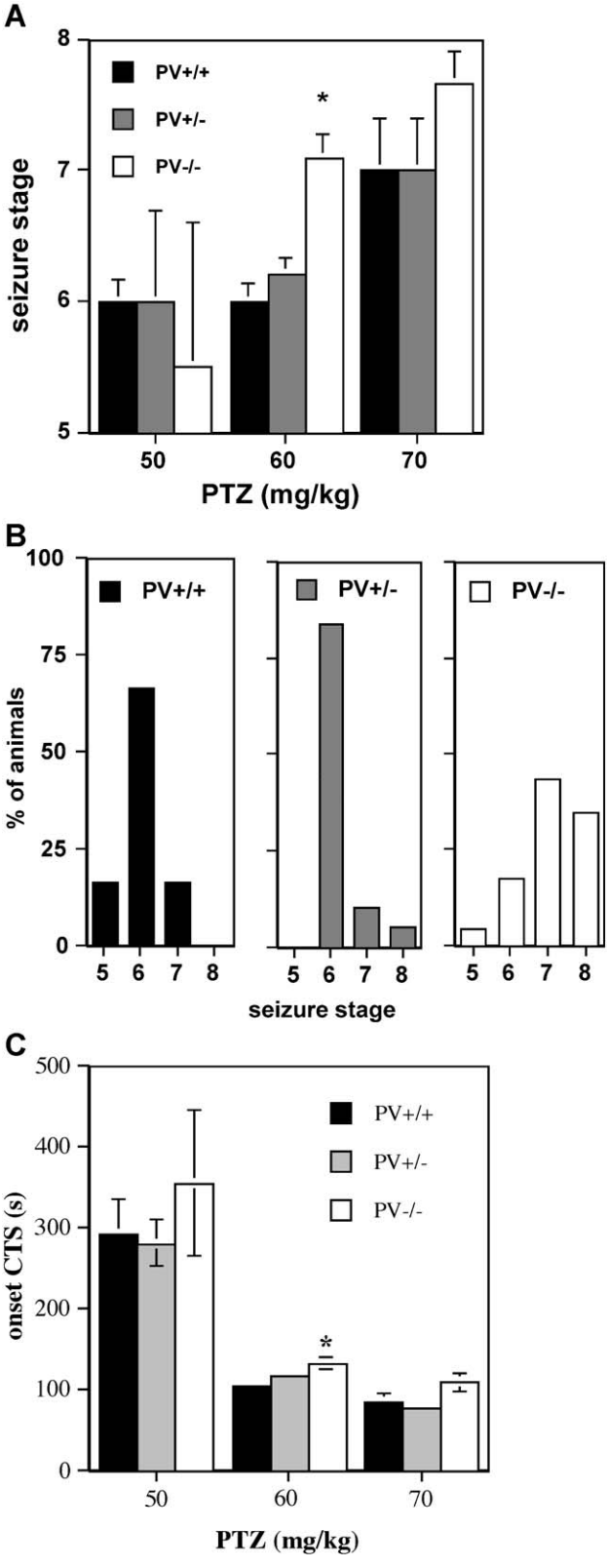

Fig. 4. (A) Seizure intensity of mice treated with convulsant doses of pentylenetetrazole (PTZ). Seizure stages (defined in Experimental methods) were determined by injection of PTZ (50, 60, or 70 mg/kg, i.p.) for the three genotypes (mean ± S. E. M.). Significant differences between the three genotypes at 60 mg/kg PTZ is corroborated by a nonparametric Kruskal–Wallis test, which showed a P value < 0.001. *Significant vs. WT; P < 0.001 using the Mann–Whitney U test. (B) For experiments with 60 mg/kg PTZ (n = 18 for PV+/+, n = 19 for PV+/− and n = 23 for PV−/−), the relative distribution of seizure stages were plotted. (C) Latency of the onset of clonic–tonic seizures (CTS) as a function of PTZ dose injected for the three genotypes. The lag period before onset is decreased with increasing doses of PTZ in all groups. PV−/− mice show a tendency to start CTS with a small delay compared to PV+/− or PV+/+ mice. At 60 mg/kg PTZ, a nonparametric Kruskal–Wallis test revealed significant differences between PV+/+, PV+/−, and PV−/− with a P value < 0.05. *Significant vs. PV+/+; P < 0.01 (Mann–Whitney U test).

The proportions of electrophysiologically characterized types of cortical neurons are changed in PV-deficient mice

In the light of the reduced seizure threshold, we have first assessed the effect of PV deficiency for neuronal networks in the neocortex. Among the interneurons that innervate pyramidal cells of the cortex, are PV-immunoreactive (PV-ir) chandelier and basket cells, which are proposed to play an important role in the

control of pyramidal cell excitability (Blümcke et al., 1990; Cauli et al., 1997; DeFelipe et al., 1989, 1993; Hendrickson et al., 1991; Hendry et al., 1989; Lewis and Lund, 1990). Thus, it is expected that any alteration in the functional properties of the PV-ir interneurones will modify local inhibition, which eventually may affect the collective activity of the whole neuronal network. Extracellular single-unit recordings from the temporal cortex were performed in Equithesin-anesthetized mice by four independently advanced microelectrodes. We analyzed the three genotypes (PV+/+, PV+/−, PV−/−, n = 6 subjects for each genotype group). Since the PV−/− strain has a mixed 129P2 × B6 background and were maintained as homozygous strains (PV+/+ and PV−/−) for several generations, a genetic drift between the two genotypes could not be excluded a priori. Thus, we included in each genotype group half of subjects with a 129SvJ background (as defined in Experimental methods). The recordings were performed along the same angle of electrode penetrations (40° off the vertical line) for all subjects. The median depths were 835, 755, and 800 μm, and the interquartile ranges 825, 855, and 825 μm in PV+/+, PV+/−, and PV−/− mice, respectively. No significant difference between the three groups could be observed with respect to the electrode depth of the recording sites. The electrode tips were mainly positioned in layers III–IV and the deepest recording of a series was largely confined to layer V according to a stereotaxic atlas of the mouse brain. A total amount of 1161 single units were recorded during spontaneous activity. The signals of 39 units changed during the experimental session and were discarded from the analysis. Recordings from an overall number of 1122 single units were analyzed (354, 397, and 371 in PV+/+, PV+/−, and PV−/− mice, respectively). The time series of the spikes—the spike trains—were analyzed by the autocorrelation technique (Abeles, 1982) and three cell types were defined by the temporal course of their discharge pattern. The 'regular' cells were characterized by a flat autocorrelogram with a trough near time zero, thus indicating a tendency to discharge following a Poisson distribution (Fig. 5a). The refractoriness (i.e., the duration of the trough near time zero measured on the autocorrelogram) of the regular spiking units was approx-

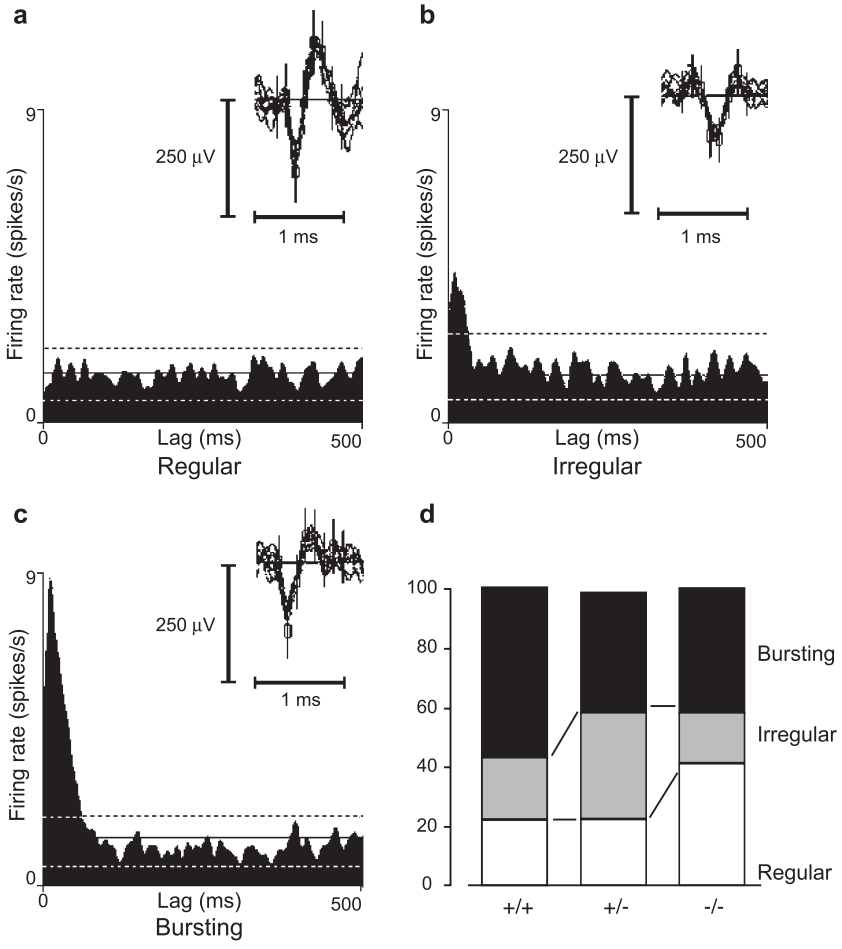

Fig. 5. Typical autocorrelograms (autorenewal density histograms) of the three types of spontaneous firing pattern observed in extracellular single-unit recordings from the temporal cortex, with lag (ms) on the abscissa and rate (spikes/s) on the ordinate. Note that abscissa is scaled to 500 ms and the ordinate is scaled to 9 spikes/s for all plots. The histograms are smoothed by a Gaussian bin of 10 ms. The average firing rate of the unit is indicated by the continuous line, whereas the broken lines correspond to 99% confidence limits following a Poisson distribution. Each autocorrelogram has an inset showing the oscilloscope traces of the corresponding extracellularly recorded single unit. (a) 'Regular' firing unit. (b) 'Irregular' firing unit. (c) Bursting firing unit, characterized by burst duration larger than 80 ms and intraburst frequency less than 30 Hz. (d) Distribution of electrophysiologically defined cell types in PV−/−, PV+/−, and PV+/+ mice. Note that in PV−/−, the proportion of "Regular" firing neurons was increased.

imately 14 ms. The remaining single units showed a tendency to fire isolated spikes intermingled with bursts, as indicated by a hump in the autocorrelogram near time zero. According to the average burst duration and intraburst frequency, it was possible to distinguish two classes of units. The first type was termed 'irregular' (Fig. 5b) and the second type, termed 'bursting' (Fig. 5c), was characterized by longer burst duration and low rate bursting, at frequencies less than 30 Hz. The average burst size was estimated by the area of the hump in the autocorrelogram (Abeles, 1982; Villa, 1990) and was about 1.7 spikes for both irregular and bursting units (the burst size is always equal to 1 in 'regular' firing units). For all groups of animals, the firing rate of both regular and bursting firing cells was statistically similar, but it was higher than the rate of discharges of irregular units (t test, $P < 0.01$).

The characteristics of the discharge pattern of all type of units were consistently the same in the three genotypes (Table 2). Conversely, the distribution of the unit types within the experimental animals was significantly different (contingency table analysis, Chi-square = 63.1, $P< 0.001$) as illustrated in Fig. 5d. The main finding is that in PV−/− subjects, the proportion of single units characterized by a regular Poisson pattern of discharges tended to be increased. On the opposite, the percentage of single units classified as bursting type was smaller in PV−/− mice. In PV+/− mice with neuronal PV levels, which are approximately one third of the ones found in PV+/+ animals (Table 1), a shift from bursting firing to irregular firing was observed. It is also interesting to note that in PV-deficient mice, the spontaneous firing rate (1.37 ± 0.08 spikes/s, average ± SEM) of all types of cells pooled together was significantly higher than in WT (1.12 ± 0.06 spikes/s) and heterozygous animals (1.10 ± 0.05 spikes/s). The comparison between PV−/− and PV+/+ in mice with a 129SvJ genetic background revealed similar results to the ones obtained in the mixed background. This suggests that the observed change from "bursting" firing to "regular" firing pyramidal neurons is likely to be the result of the deletion of the functional PV gene and not due to differences in the genetic background of PV+/+ and PV−/− mice with the mixed B6x129P2 genetic background. The influence of the genetic background in different knockout strains has been discussed in great detail (Gerlai, 1996; Zimmer, 1996) and is principally concerned with behavioral differences of different strains. Nonetheless, also electrophysiological recordings in vivo might be susceptible to variations of the genetic background, but the similar results we have obtained with the two PV−/− lines is in support of an effect due deletion of the functional PV gene.

PV deficiency promotes depolarizing IPSCs in hippocampus

We next assessed the effect of PV deficiency on neuronal networks in the epilepsy prone hippocampus. Hippocampal PV interneurons are organized in a network of interconnected cells and are thought to significantly affect network properties (Bartos et al., 2002; Fukuda and Kosaka, 2000). It has been previously demonstrated that PV-deficiency facilitated repetitive IPSCs and related inhibition-based gamma oscillations in the hippocampus (Vreugdenhil et al., 2003). Here, we recorded monosynaptic $GABA_A$ergic IPSCs in hippocampal slices evoked by stimulation of the near stratum pyramidale. Under our experimental conditions, the postsynaptic responses were completely blocked by 50 μM bicuculline methiodide and therefore mediated by $GABA_A$ receptors (data not shown). At maximal IPSP stimulus intensity, the $GABA_A$ergic IPSC had shown a late current reversal (Vreugdenhil et al., 2003). At this intensity, a train of 20 pulses at 100 Hz induced a hyperpolarization followed by a massive slow depolarization in cells recorded in current clamp mode (Fig. 6A). The addition of the $GABA_A$ receptor antagonist bicuculline methiodide (50 μM) completely blocked the slow depolarization (Herrero et al., 2002) and unmasked a depolarization associated with the stimulus train (four out of four cells from three control mice tested), which in turn was blocked by the metabotropic glutamate receptor group I antagonist (*S*)-3-carboxy-4-hydroxyphenylglycine (50 μM; Fig. 6A). The maximum depolarization was 14.2 ± 2.6 mV for seven cells from six PV−/− mice and 9.3 ± 2.4 mV for nine cells from seven PV+/+ mice (n.s.). The slow depolarization evoked action potential trains in five out of seven (71%) cells from PV−/− vs. three out of nine (33%) cells from PV+/+. In voltage-clamp mode, the cells responded with a sustained inward current following an initial outward current, which was blocked by bicuculline (Fig. 6B), indicating that current reversal is mainly due to bicarbonate efflux after collapse of the chloride gradient (Davies and Collingridge, 1993; Kaila, 1994). We have not further explored the contribution of a GABA activity-dependent potassium transient to the late phase of the depolarization (Bracci et al., 1999; Kaila et al., 1997). The contribution of the small remaining metabotropic glutamate receptor group I-sensitive inward current (Congar et al., 1997) was restricted to the duration of the tetanic stimulus (Fig. 6B). Despite the relatively small first outward IPSC (−0.6 ± 0.2 nA vs. −0.9 ± 0.3), the peak amplitude of the slow inward current in PV−/− cells did not differ significantly from that for PV+/+ cells (0.8 ± 0.1 nA. vs. 0.5 ± 0.1 nA; $P< 0.09$). But more importantly, the reversal of the IPSC occurred significantly earlier in cells from PV−/− mice (255 ± 34 ms after the onset of the

Table 2
Spontaneous activity parameters of cortical units grouped according to the temporal pattern of discharges (median, mean ± SEM)

Type	Genotype	N	Firing rate (spikes/s)	Average burst duration (ms)	Average burst size (spikes)	Intraburst frequency (Hz)	Bursting index (Hz)
Regular	PV+/+	79	0.7 (1.3 ± 0.2)	10.0[a] (16.2 ± 2.2)	–	–	–
	PV+/−	92	0.9 (1.1 ± 0.1)	10.0[a] (14.8 ± 2.4)	–	–	–
	PV−/−	151	0.9 (1.4 ± 0.2)	10.0[a] (12.0 ± 0.9)	–	–	–
Irregular	PV+/+	76	0.5 (0.8 ± 0.1)	30.0 (45.4 ± 5.5)	1.3 (2.0 ± 0.3)	40.9 (45.7 ± 1.8)	0.8 (1.1 ± 0.1)
	PV+/−	140	0.6 (0.9 ± 0.1)	30.0 (34.8 ± 1.6)	1.4 (1.7 ± 0.1)	50.6 (53.0 ± 1.5)	0.7 (0.8 ± 0.1)
	PV−/−	84	0.8 (1.2 ± 0.2)	30.0 (37.8 ± 3.0)	1.3 (1.7 ± 0.1)	42.5 (47.8 ± 1.8)	0.8 (0.9 ± 0.1)
Bursting	PV+/+	199	0.8 (1.2 ± 0.1)	90.0 (89.5 ± 2.9)	1.5 (1.6 ± 0.1)	18.6 (19.3 ± 0.4)	4.5 (5.6 ± 0.3)
	PV+/−	165	1.0 (1.3 ± 0.1)	95.0 (98.5 ± 4.0)	1.6 (1.8 ± 0.1)	19.1 (19.5 ± 0.5)	4.6 (6.4 ± 0.5)
	PV−/−	132	1.1 (1.4 ± 0.1)	90.0 (96.4 ± 4.3)	1.4 (1.6 ± 0.1)	18.6 (18.9 ± 0.5)	4.8 (6.4 ± 0.5)

[a] For the 'regular' firing units, this duration corresponds to the refractory period.

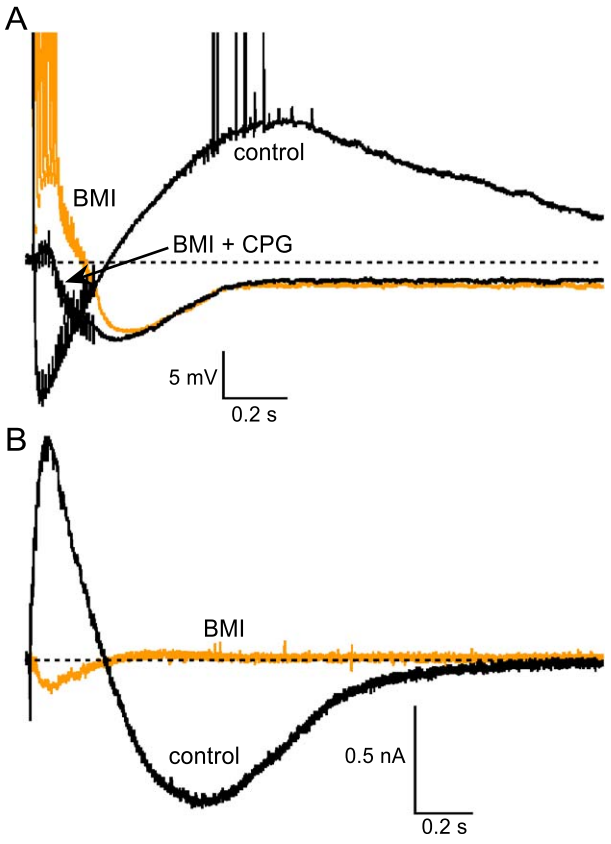

Fig. 6. Facilitated $GABA_A$ergic current reversal with high-frequency stimulation. (A) The response of a CA1 hippocampal neuron from a PV+/+ mouse to tetanic stimulation (20 pulses at 100 Hz) at maximal IPSP stimulus intensity recorded in current clamp in standard solution, in the presence of the $GABA_A$ receptor antagonist bicuculline methiodide (BMI; 50 μM) and after addition of the metabotropic glutamate receptor group I antagonist (*S*)-3-carboxy-4-hydroxyphenylglycine (CPG; 50 μM). Tetanic stimulation evokes a late slow $GABA_A$ergic depolarization, triggering repetitive firing. The early $GABA_A$ergic hyperpolarization masks a metabotropic glutamate receptor-mediated depolarization. (B) Under voltage-clamp conditions, tetanic stimulation causes a slow inward current following an outward current in standard solution. Bicuculline (BMI; 50 μM) unmasks a small inward current that is restricted to the duration of the tetanic stimulus.

stimulus train vs. 377 ± 51 ms, Student's *t* test $P < 0.05$). Thus, PV deficiency accelerates the $GABA_A$ergic current reversal induced by high-intensity, high-frequency stimulation.

Discussion

Expression of other CaBPs, neurotransmitter receptors, and morphology of "PV neurons" in PV−/− mice

In recent years, a wealth of work has been published on the distribution of particular calcium-binding proteins including PV, CB, and calretinin (CR) (for a review, see Andressen et al., 1993; Baimbridge et al., 1992; DeFelipe, 1997), but much less is known about the functional significance of these proteins. Although their affinities for Ca^{2+} are all in the submicromolar range, they are expressed in distinct, mainly nonoverlapping populations of neurons suggestive of specific functions. Ideas about these "specific" functions remain relatively vague and include such general functions as involvement in Ca^{2+}-buffering, Ca^{2+} homeostasis and also are role in the protection against excitotoxicity has been proposed, but results on the latter aspect are controversial (e.g., Hartley et al., 1996; Klapstein et al., 1998; Meier et al., 1997). Within the last years, knockout mice for the three proteins PV (Schwaller et al., 1999), CB (Airaksinen et al., 1997), and CR (Schiffmann et al., 1999) have become available and have been used to address some of these questions (Schwaller et al., 2002). Interestingly, the expression patterns of the other two proteins in either CB−/− (PV, CR) or CR−/− (PV, CB) mice were not significantly changed and also global expression levels determined by Western blot analysis were not altered. These results are in good agreement with our findings that neither the distribution nor the levels of CR and CB were affected by the lack of PV. This suggests that at least at the level of these three proteins, no compensatory mechanism is induced by the lack of either one of these. Furthermore, the lectin staining of the "perineuronal" nets—a characteristic accumulation of extracellular matrix molecules in intimate contact with the surface of PV-expressing neurons (Celio and Blümcke, 1994)—with either VVA (this report) or *W. floribunda* agglutinin (WFA) (Haunso et al., 2000) revealed the "PV neurons" to be present in the neocortex. Neither analysis at the global level (this report), in the hippocampus (Vreugdenhil et al., 2003), nor in refined detail by fluorescence microscopy (Haunso et al., 2000) revealed any differences of the perineuronal nets in PV−/− mice, suggesting morphologic and metabolic entireness of these neurons. These findings were additionally supported by the identification of fast-spiking (FS) cells in the PV-deficient mice, which also indicates an intact functional activity. In summary, all the available information suggest that the lack of the slow-onset Ca^{2+}-buffer PV does not substantially affect the distribution, morphology, and basic electrophysiological properties of the subpopulation of cortical interneurons normally expressing PV. These findings are in excellent agreement with previous ones on the cytoarchitecture of the hippocampal formation in PV−/− mice, where no differences in the number, distribution, or morphology of interneurons compared to wild-type mice were observed (Bouilleret et al., 2000). Quantitative analysis of the number of VVA-positive cells per length of pyramidal layer revealed these not to be different between PV+/+ and PV−/− mice (Vreugdenhil et al., 2003). Additionally, immunohistochemistry for the $GABA_A$ receptor subunits α1, α2, and β2/3 showed no apparent differences when comparing neocortical regions of PV−/− and PV+/+ mice (J.-M. Fritschy, personal communication). This is line with our results from semiquantitative Western blots using different antibodies against $GABA_A$ receptor subunits. Analysis of $GABA_A$ receptor subunit mRNA levels by DNA chip technology also revealed no significant differences between genotypes in cerebellum and forebrain. In these experiments, no changes in abundance of other neurotransmitter receptor mRNAs including different types of glutamate receptors or peptide receptors were observed (data not shown). Although subtle changes at the level of $GABA_A$ receptors cannot be entirely excluded, we currently do not have any indications for such changes in PV-deficient mice. In addition, we cannot rule out the possibility that differential expression could take place only in a subpopulation of cells and would not be detected in complex tissues such as forebrain or cerebellum.

PV deficiency and susceptibility to epileptic seizures

PTZ-induced seizure onset is known to be localized in deep brain structures spreading to the hippocampus and neocortex (Binnie et al., 1985). Thus, hippocampus and neocortex are involved in seizure spread and its behavioral expression rather than in seizure initiation. Although there were no differences at low doses of PTZ and the time interval until onset of clonic–tonic seizures was longer in PV-deficient mice, the seizures were more severe. This suggests that these mice display facilitated seizure spread in cortical areas despite an increased threshold to seizures in these areas. Previously, we did not notice a change in the expression of kainate-induced seizures in PV−/− mice (Bouilleret et al., 2000), but since a detailed morphological analysis was the principal aim of this study, no electroencephalogram analysis was carried out. The relation between PV and epilepsy has been established in various studies. Evidence was provided that PV is lost from GABAergic perikarya of adult gerbils with repeated clonic–tonic seizures, while gerbils showing no seizure activity retain a high number of PV neurons in the CA1 region of the hippocampus (Scotti et al., 1997). Multiple small regions with abnormal patterns of immunostaining for PV and glutamic acid decarboxylase (GAD) have been observed in human neocortex resected during surgical treatment of intractable temporal lobe epilepsy (Marco et al., 1996). In these patients, the PV immunoreactivity of GAD-ir neurons was reduced, a finding that is compatible with at least two interpretations: (i) the disappearance of neurons normally expressing PV or (ii) down-regulation of PV in this cell population. If the latter one is assumed and since PV-ir GABAergic neurons include chandelier cells and basket cells that exert powerful regulation of impulse generation in cortical pyramidal cells (DeFelipe, 1999), this might implicate that in the absence of PV crucial perisomal inhibition is increased in these networks. In the hippocampus of rats subjected to two experimental models of temporal lobe epilepsy (TLE), Cossart et al. (2001) reported that dendritic GABAergic inhibition was reduced likely due to the loss of a subgroup of interneurons (O-LM cells), which project on the distal dendritic tree of principal cells. On the other hand, perisomatic projecting interneurons (presumably PV-ir basket cells) remained intact and were found to be hyperactive in that model of TLE. The authors proposed that the increased somatic inhibition could provide a means to keep the network under the control most of the time. Interestingly, this idea has been challenged in several reports, where an increased rather than a decreased inhibition was detected (Otis et al., 1994; Prince and Jacobs, 1998). Theoretical analysis suggests that an increase of inhibition in networks of interneurons contributes to synchronization of their firing and that of principal cells (Di Garbo et al., 2002). In a mathematical model of layer V cortical neurons, Bush et al. (1999) "induced" epileptiform activity by increasing pyramidal cell excitability, which was often paralleled by increased perisomatic inhibition. Increased inhibition was actually observed experimentally in postlesional epileptogenic slices (Prince et al., 1997) supporting the "counterintuitive" hypothesis of increased inhibition facilitating ictogenesis. This is in line with previous findings that GABA or GABA-enhancing substances can induce epileptiform activity (Kaila et al., 1997; Lopantsev and Avoli, 1998). Also, in other epilepsy models, GABA-mediated inhibition is increased (Traub et al., 1996). Interestingly, increasing GABA release with a $GABA_B$ receptor antagonist, which increases GABAergic depolarizations (Bracci et al., 1999), aggravates PTZ-induced seizures (Veliskova et al., 1996). The slightly delayed onset of the clonic–tonic seizures is also in line with a stronger inhibition. While in cortical areas, a slight reduction of inhibition can cause epileptiform activity (Whittington et al., 1995), a stronger inhibition may delay the point where PTZ disables inhibition beyond that critical level.

Lack of PV and firing pattern of cortical pyramidal neurons

Our PTZ results show that the absence of PV is correlated with a modification of the inhibitory functions normally exerted by nonpyramidal cells of the temporal neocortex. An in vitro analysis of layer V cortical cells in the rat revealed different electrophysiologically defined classes including regular spiking cells (RS_1 and RS_2) and intrinsically bursting cells (IB) based on action potential firing in response to current injection (Hefti and Smith, 2000). A strict definition of RS_1, RS_2, and IB cells was not always possible and the authors proposed the existence of a kind of continuum of firing properties with RS_1 an IB cells being the extreme on the scale. In our in vivo electrophysiology experiments, we defined three categories of cells based on their spontaneous firing pattern as regular, irregular, or bursting cells with a likely correlation to RS_1, RS_2, and IB cells, respectively. While in the complete absence of PV in PV−/− mice, a shift in the proportion of cells with bursting firing characteristics to regular firing ones was observed, the reduced amount of PV in the PV+/− neurons had an intermediate effect indicative of a gene-dosage effect. This is reflected by the increased proportion of irregular firing cells, while the decrease in the proportion of bursting firing cells was much less pronounced than in PV−/− animals.

How can we reconcile the differences in firing properties of pyramidal cells and the increased control of inhibition in PV−/− mice? (i) According to Hefti and Smith (2000), IB cells are characterized by their greater ability to fire short bursts of action potentials in response to thalamocortical stimulation and the amount of inhibitory input is much smaller than in RS cells. Thus, an increase in the ratio of RS vs. IB cells could be interpreted as an increase in inhibition. (ii) Pharmacological experiments using the $GABA_A$ receptor agonist muscimol and the benzodiazepine receptor agonist flurazepam in combination with electrophysiological recordings from the somatosensory cortex of anesthetized rats (Oka et al., 1993) revealed two distinct firing patterns (regular spiking and bursting). Inhibition of cells characterized by bursting pattern of firing was significantly weaker than in cells displaying the regular spiking pattern. (iii) Our previous experiments on short-term plasticity with PV−/− mice, i.e., facilitated paired-pulse modulation between PV-ir basket and Purkinje cells in the cerebellum (Caillard et al., 2000) and facilitated repetitive IPSCs at frequencies >20 Hz in the hippocampus (Vreugdenhil et al., 2003), are all in support of increased inhibition in the absence of PV. The highest density of PV-ir neurons and innervation in the rodent neocortex is in layers III–V (for a review, see Hof et al., 1999), the region where most of the in vivo extracellular activity presented here was recorded. Thus, the decreased ratio of bursting cells in PV−/− subjects observed in our extracellular electrophysiological recordings is in agreement with the above-mentioned studies and may well be associated with increased local inhibitory effects due to the lack of PV in GABAergic cells. It cannot be excluded that other secondary not yet identified effects resulting from the inactivation of the PV gene may also contribute to the observed

changes in the proportions of pyramidal cells with distinct firing patterns.

Increased inhibition and network effects

Although intuitively facilitated GABA release is not expected to be epileptogenic, when GABAergic inhibition is challenged, it can turn into a depolarizing driving force, involved in seizure initiation (Fujiwara-Tsukamoto et al., 2003; Kohling et al., 2000). In the present study, we observed that in hippocampal slices, the $GABA_A$ergic current reversal induced by high-frequency stimulation of the IPSC occurred significantly earlier in cells from PV−/− mice compared to wild-type controls. These so-called GABA-mediated depolarizing postsynaptic potentials (Kaila et al., 1997) previously reported in CA1 pyramidal cells evoked by high-frequency stimulation are characterized by their large amplitude and prolonged duration. In the rat entorhinal cortex, 4-AP-induced NMDA-dependent synchronous activity leading to ictal-like epileptiform discharges have been demonstrated to be mediated via a $GABA_A$ergic mechanism (Lopantsev and Avoli, 1998). Furthermore, depolarizing GABA responses were observed in slices of human cortical tissue from epilepsy surgery (Deisz, 2002) and were also shown to contribute to intericatal activity in human temporal lobe epilepsy (Cohen et al., 2002). Here we report that PV deficiency facilitates the proconvulsive GABA-mediated depolarizing postsynaptic potential in the hippocampus. Due to the similarity of the hippocampal and neocortical network of PV-ir neurons with respect to GABAergic projections to pyramidal neurons exerted by these neurons—and also based on previous ultrastructural, immunohistochemical, and functional data—we propose that this facilitation may occur in the neocortex as well, although this remains to be proven. In support of this hypothesis are the findings that short-term modulation was facilitated in the absence of PV, both in the cerebellum (Caillard et al., 2000) and hippocampus (Vreugdenhil et al., 2003), indicating that PV has a similar function in the different interneuron populations.

Model of the role of PV in neuronal networks

The assumption that PV deficiency is likewise manifested in both in vitro and in vivo recordings of hippocampal and neocortical pyramidal neurons, respectively, and data from previous in vitro studies on the Ca^{2+} buffering properties and the deduced function of PV have led us to propose the following model. Delayed Ca^{2+} buffering by PV helps to increase the initial decay of $[Ca^{2+}]_i$ in presynaptic PV-containing terminals. In its absence, residual $[Ca^{2+}]_i$ remains elevated for longer periods, which favors short-term facilitation at relatively short (<50 ms) interspike intervals. In PV−/− mice, increased facilitation is translated into increased inhibition in networks consisting of normally PV-containing interneurons and pyramidal cells. This, in turn, shifts the firing properties of a fraction of pyramidal cells from "bursting" to a "regular" firing pattern. Such "regular" discharge pattern in the cerebral cortex is associated to a coincidence-detector mode of functioning of pyramidal cells (Abeles, 1991). In this mode, the pyramidal cell is able to generate an action potential because the gain of several synchronous EPSPs is much larger than the sum of their asynchronous inputs. That is, less input, which is synchronized in time, is more effective and tends to be transmitted through the cerebral network with synchronous volleys (Diesmann et al., 1999). Preliminary analyses of local field potentials in PV-deficient mice indicate a tendency to an increased area of synchronization (Villa et al., 2000). We propose that the shift in the firing pattern observed in the PV−/− mice increases the probability of activating synchronous firing over a larger area and thus to an increased susceptibility toward epileptogenic insults such as the ones induced by PTZ.

In conclusion, we suggest that the absence of PV in the subpopulation of GABAergic interneurones modifies the dynamics of the inhibitory control at the local level. Although the extent of this modification may vary in brain-region-specific PV-ir populations, we may postulate the following generalized hypothesis: During normal spontaneous activity, this change in the dynamics of the inhibitory control leads to an increase in inhibition. However, when networks are further challenged by inputs that affect cellular excitability, the facilitated inhibition may turn into a depolarizing force, allowing hypersynchronous neuronal activity to propagate over larger networks, thus facilitating seizure initiation and/or spreading.

Experimental methods

Generation of PV-deficient mice and breeding

Mice with two different genetic backgrounds were used in this study. The first group of mice are a mixed background of 129/OlaHsd × C57BL/6J (129P2 × B6) and are named PV−/−. In the second group, the chimeric mice derived from injection of targeted embryonic stem cells (E14/Ola; Hooper et al., 1987) in the blastocysts of C57BL/6J mice were mated to 129/SvEv mice resulting in the 129PV−/− line (129/OlaHsd × 129/SvEv). Electrophysiological experiments were carried out with both groups of mice. In the PTZ studies, besides the WT animals with a mixed 129/OlaHsd × C57BL/6J background, a F1 generation between 129/SvEv and C57BL/6J mice were bred and were not found to be significantly different from the PV+/+ mice in this assay. Biochemical analysis (Western blot, ELISA) and immunohistochemistry was performed with the 129/OlaHsd × C57BL/6J (PV−/−) mice.

PCR analysis for genotyping

From all mice used in the experiments, a small tail biopsy (2–3-mm long) was taken and genomic DNA was isolated using a commercial kit (Invitrogen, Groningen, The Netherlands) and 300 ng of purified DNA were used per PCR reaction. For the genotyping of the animals, two PCR reactions were carried out. The strategy makes use of the fact that in the mutated allele, the majority of the coding sequence has been replaced by a neocassette (Schwaller et al., 1999). Amplification of exon 3 gives rise to a fragment of 151 bp, while amplification of a part of the neoresistance leads to one of 188 bp. The former confirms the presence of a wild-type allele and the latter a mutated one. The PCR protocol used is the following: 94 °C for 2 min, 72 °C for 10 s [addition of Taq Polymerase (DyNAzyme II, Bioconcept, Allschwil, Switzerland) at this point], followed by 40 cycles (94 °C for 20 s, 68 °C for 40 s, and 72 °C for 40 s).

Immunohistochemistry

Immunohistochemical analysis of floating cryostat brain sections (40 μm thickness) was performed as described by Celio and Heizmann (1982), with the exception that the bound primary antibody was revealed by the avidin–biotin technique instead of

the peroxidase–anti-peroxidase one. For immunostaining, the following antibodies were used: anti-parvalbumin PV4064 (1:5000; Swant, Bellinzona, Switzerland), anti-calbindin D-28k CB300 (1:5000; Swant), and anti-calretinin CR7696 (Schwaller et al., 1993). The perineuronal nets around parvalbumin-expressing neurons were visualized with peroxidase-labeled isolectin B4 *V. villosa* agglutinin (VVA, Sigma L-5641, Buchs, Switzerland) as described (Lüth et al., 1992).

Western blot detection of PV in the forebrain and cerebellum

The brains were removed from sacrificed mice and separated into forebrain and cerebellum, and Western blots performed with the same antibodies against PV, CB, and CR as above as previously described (Schwaller et al., 1993).

Semiquantitative Western blot analysis of $GABA_A$ receptor subtypes

Forebrain samples were homogenized and 60 μg (α2, α3) or 20 μg (β2/3) of total protein extract were separated by SDS-PAGE (10% PAA gels). Proteins were transferred to blotting membranes and probed with antibodies against α2, α3, and β2/3 $GABA_A$ receptor subunits as described before (Mohler et al., 1995) (kind gift from J.-M. Fritschy, University of Zurich, Switzerland).

ELISA

Quantitative results on PV content in the forebrain and cerebellum of WT, PV+/−, and PV−/− mice were obtained by a sandwich-ELISA method. The procedure for PV (Caillard et al., 2000) is essentially the same as for the detection of CR as described in detail previously (Schierle et al., 1997). Briefly, for the coating of the ELISA plates, the monoclonal antibody PV235 is used and the bound PV is detected by the polyclonal rabbit antiserum PV4064. All samples were measured in triplicates and samples were taken from two animals of each genotype.

Electrophysiological recordings in vivo

The genotype of all tested animals was revealed to the experimenter only after measurements were done and calculations had been performed. The animals (six of either genotype, 32.8 g body weight on average) were anesthetized with an i.p. injection of Equithesin (0.035 ml/g body weight) at a dose corresponding to 130 mg/kg chloral hydrate and 30 mg/kg of pentobarbital. Equithesin was prepared from a solution of chloral hydrate and pentobarbital sodium (Li and Kelly, 1992) and was shown to preserve subtle response patterns in the auditory midbrain (Li and Kelly, 1992). The animals were mounted in a stereotaxic apparatus without ear bars. The limb withdrawal reflex was checked regularly to monitor the depth of anesthesia. Body temperature was monitored permanently and maintained between 37°C and 39°C with a heating pad. Four to five independently driven tungsten-glass insulated microelectrodes were advanced stepwise in the temporal cortex (Villa et al., 1999). We aimed to be nearly perpendicular to the surface of the temporal cortex and the angle of penetration of the electrodes was set to 40° with respect to the vertical line. Generally, six sets of recordings were performed in one mouse, the first one in layer II, a majority (four) in layers III and IV, and the last one in layer V. Whenever electric signals corresponding to good extracellular spikes were observed, the procedure to sort single units from one electrode signal was started with a commercial device (MultiSpike Detector, Alpha Omega Engineering) based on digital signal processing and an on-line template matching algorithm to detect and sort spike waveforms. Up to three different extracellular waveforms (reflecting discharges of three distinct neurons) were discriminated from each microelectrode, with a maximum number of 15 cells being recorded per cell group. The electric impedance of our microelectrodes was about 1–2 MΩ, an unfavorable value to record the extracellular electric fields generated by small neurons. On the basis of our experience, we assume that the population of extracellular recorded units corresponded mainly to pyramidal cells and no systematic bias in recording particular cell types in the different genotypes are expected. After isolation of 10–15 single units, a recording session lasting approximately 1 h was started. The spike firing times of each unit were given by interrupts generated by a digital acquisition board (National Instruments NB-32F) driven by an external clock with an accuracy of 1 ms and stored digitally for off-line analyses. Time domain analyses including autocorrelation histograms (Perkel et al., 1967a,b) were calculated from the time series formed by the spike firing times (i.e., the spike trains) using established methods (Abeles, 1982).

Electrophysiology in vitro

Adult mice, randomly selected from both groups (PV+/+ and PV−/−) and from controls, were anaesthetized by intraperitoneal injection of a ketamine (75 mg kg^{-1})/medetomidine (1 mg kg^{-1}) mixture and then killed by cervical dislocation. The brain was quickly removed from the skull and chilled in ice-cold artificial cerebrospinal fluid (aCSF). The composition of the aCSF was (in mM): NaCl 125; KCl 3; $NaHCO_3$ 26; NaH_2PO_4 1.25; $CaCl_2$ 2; $MgCl_2$ 1; D-glucose, 10; pH was equilibrated at 7.4 with a 95% O_2/5% CO_2 gaseous mixture. For the recording of $GABA_A$ergic responses, the brain was cut into 400-μm-thick transverse slices, using a Vibroslice (Campden Instruments Ltd. Sileby, UK). Slices were transferred to a recording chamber (sustained at 33°C), wherein they were maintained at the interface between a warm moist gaseous atmosphere (95% O_2/5% CO_2) and aCSF, flowing at a rate of 2 ml/min. The aCSF was supplemented with 20 μM 6-Nitro-7-sulphamoylbenz[*f*]quinoxaline-2,3-dione (NBQX), 25 μM D-2-amino-5-phosphonovaleric acid (APV), 1 μM CGP 55845A, 5 μM atropine sulphate, and 5 μM naloxone hydrochloride to isolate $GABA_A$ergic responses and minimize presynaptic suppression by $GABA_B$ receptors (Davies and Collingridge, 1993; Lambert and Wilson, 1994), muscarinic receptors (Hajos et al., 1998), and μ opioid receptors (Lambert et al., 1991), respectively. To promote facilitation (Lambert and Wilson, 1994; Thomson, 1997), the release probability was reduced by increasing the concentration of $MgCl_2$ to 3 mM. Brain slices were allowed to equilibrate for 1 h before the onset of recording. Monosynaptic $GABA_A$ergic responses were evoked by electrical stimulation (0.1-ms square pulse) using a constant voltage stimulus isolator (Digitimer, Welwyn Garden City, England). The stimulus was applied with a bipolar electrode, constructed from a pair of insulated and intertwined 50-μm-diameter nickel/chromium wires (Advent Research Materials Ltd., Halesworth, UK), placed in the pyramidal cell layer of area CA1b, within 0.1 mm from the recording site. Intracellular current-clamp and single-electrode voltage-clamp recordings were taken from neurons within the stratum pyramidale using sharp

pipettes filled with 2 M potassium methylsulphate (tip resistance was 50–70 MΩ) connected to an Axoclamp-2A amplifier (Axon Instruments, Burlingham, CA, USA). Impaled cells were first inspected in current-clamp and accepted for recording when the resting membrane potential was at least −55 mV and when the current injection-induced overshooting action potentials. For current-clamp recordings, the resting membrane potential was manually adjusted to −65 mV. Single-electrode switch voltage-clamp recordings were accepted when the switching rate was >4 kHz and voltage clamp efficiency was >90%, as judged from the difference in the inhibitory postsynaptic potential (IPSP) amplitude between voltage-clamp and current-clamp recordings. The holding potential was −65 mV. Single- and double-pulse stimulations were applied at 15-s intervals and stimulus trains (10 pulses) were applied at 3-min intervals.

NBQX, APV, naloxone hydrochloride, atropine sulphate and (*S*)-3-carboxy-4-hydroxyphenylglycine (CPG) were obtained from Tocris–Neuramin (Bristol, UK), Signals were band-pass filtered (1 Hz–3 kHz) and sampled at a rate of 10 kHz using a CED 1401 interface and Signal software (Cambridge Electronical Design Ltd., Cambridge, UK). Current traces were digitally filtered off-line. The power of the oscillations was measured by performing fast Fourier transformations over five consecutive 10-s traces. Cross-correlation analysis between field potentials was made over five consecutive traces, using Spike2 software (Cambridge Electronic Design Ltd., Cambridge, UK).

PTZ experiments

Experiments were carried out according to the NIH guidelines for the Care and Use of Laboratory Animals, the European Committee Council Direction of November 24, 1986 (86/69/EEC), and in accordance with the Veterinary Office of the Canton of Fribourg, Switzerland. The number of animals used in the PTZ experiments was kept to an absolute minimum. A total of 117 male and female adult mice were used in this study; 36 PV+/+, 31 PV+/−, 34 PV−/− mice, and 16 F1 129/SvEv × C57BL/6J WT animals. Seizures were induced by convulsant doses of PTZ (Sigma; 50–70 mg/kg i.p.) and numbers of animals (PV+/+, PV+/−, PV−/−) that were tested with different doses of PTZ are the following: at 50 mg PTZ (12, 6, 5), at 60 mg (18, 19, 23) and at 70 mg (6, 6, 6), respectively. The genotype of mice for testing seizure susceptibility was masked until the end of experiments. The seizure intensity was recorded using the following scale: (1) decreased locomotor activity; (2) twitching either of the whole body or localized; (3) 1–20 myoclonic body jerks during the 10-min period; (4) more than 20 myoclonic body jerks during the 10-min period; (5) clonic forelimb convulsions; (6) generalized tonic–clonic seizures, characterized by forelimb and/or hindlimb clonus and tonus resulting in episodes of falling down; (7) status epilepticus (SE); (8) death. Similar scaling of PTZ-induced seizure intensities in mice has been reported before (Ferraro et al., 1999). Animals were observed during a 20-min period. The latency of onset of clonic–tonic seizures was recorded as well as the mortality rate.

Statistics

The firing parameters (sample sizes consisting of the extracellular recorded units varied between $n = 76$ and $n = 199$) followed Gaussian distributions (Kolmogorov–Smirnov test) and were analyzed by Student's t test. The distribution of unit types (bursting, regular, irregular) within experimental groups was evaluated by contingency table analysis (Chi-square test) and the significance level was set at $P < 0.01$. In the PTZ experiments, differences between the three genotypes at 60 mg/kg PTZ were corroborated by a nonparametric Kruskal–Wallis test and P values < 0.05 were considered significant. For comparison between two genotypes, the Mann–Whitney U test was used and differences were considered significant at $P < 0.05$.

cDNA microarray analysis

Microarray analysis was performed from mRNA extracted from 3 to 6 months old male mice using the one-step method Fastrack (Invitrogen). To reduce interindividual variability, each genotype was constituted by pools of tissues from five different mice. DNA microarray technology was performed on microscope polylysine-coated slides using the technology developed by Patrick Brown at Stanford (Eisen and Brown, 1999; Schena et al., 1995) and adapted at ESPCI (Potier et al., 2002). The list of genes present on the array can be found at http://www.bio.espci.fr/~puces/neuropuces.html. Briefly, PCR products were spotted on polylysine-coated slides using the Omnigrid from Genemachine (California) with MicroQuill 1000 (Majer Precision, Inc.). Microarrays were hybridized with fluorescent targets obtained by reverse transcription of mRNA from PV−/− and PV+/+ littermates cerebella and forebrains at 60°C in 3.4× SSC, 0.28% SDS overnight. After washing, the slides were scanned on the General Scanning (Scanarray 3000) capable of analyzing Cy3 and Cy5 fluorescence on spots at a resolution of 10 μm per pixel. Scanned images were then analyzed with the image analysis software Imagene 4.1 (Biodiscovery Inc.). Data were normalized using either a lowess fit or a linear regression on a set of control genes. Statistical analysis was performed using VARAN and the error model generated from control experiments (NT lowess 0.99, P= 0.01 in Varan Analyzer; http://www.bionet.espci.fr/varan/varan_info.html; Golfier et al., 2004).

Acknowledgments

We would like to thank S. Eichenberger, Fribourg, for taking care of the animal facilities and B. Belser, Fribourg, for excellent technical support in histochemical methods. The project was supported by the Swiss National Science Foundation (grant 3200-059559.99/1 to M.R.C. and grants 3100-063448.00/1 and 3100A0-100400/1 to B.S.) and Novartis.

References

Abeles, M., 1982. Quantification, smoothing, and confidence limits for single-units' histograms. J. Neurosci. Methods 5, 317–325.

Abeles, M., 1991. Corticonics: Neural Circuits of the Cerebral Cortex. Cambridge Univ. Press, Cambridge, p. 280.

Airaksinen, M.S., Eilers, J., Garaschuk, O., Thoenen, H., Konnerth, A., Meyer, M., 1997. Ataxia and altered dendritic calcium signaling in mice carrying a targeted null mutation of the calbindin D28k gene. Proc. Natl. Acad. Sci. U. S. A. 94, 1488–1493.

Aird, R.B., Gordon, N.S., 1993. Some excitatory and inhibitory factors involved in the epileptic state. Brain Dev. 15, 299–304.

Andressen, C., Blümcke, I., Celio, M.R., 1993. Calcium-binding proteins: selective markers of nerve cells. Cell Tissue Res. 271, 181–208.

Baimbridge, K.G., Celio, M.R., Rogers, J.H., 1992. Calcium-binding proteins in the nervous system. Trends Neurosci. 15, 303–308.

Bartos, M., Vida, I., Frotscher, M., Meyer, A., Monyer, H., Geiger, J.R., Jonas, P., 2002. Fast synaptic inhibition promotes synchronized gamma oscillations in hippocampal interneuron networks. Proc. Natl. Acad. Sci. U. S. A. 99, 13222–13227.

Bernard, C., Hirsch, J.C., Ben-Ari, Y., 1999. Excitation and inhibition in temporal lobe epilepsy: a close encounter. Adv. Neurol. 79, 821–828.

Binnie, C.D., Van Emde Boas, W., Wauquier, A., 1985. Geniculate spikes during epileptic seizures induced in dogs by pentylenetetrazol and bicuculline. Electroencephalogr. Clin. Neurophysiol. 61, 40–49.

Blümcke, I., Hof, P.R., Morrison, J.H., Celio, M.R., 1990. Distribution of parvalbumin immunoreactivity in the visual cortex of old world monkeys and humans. J. Comp. Neurol. 301, 417–432.

Bouilleret, V., Schwaller, B., Schurmans, S., Celio, M.R., Fritschy, J.M., 2000. Neurodegenerative and morphogenic changes in a mouse model of temporal lobe epilepsy do not depend on the expression of the calcium-binding proteins parvalbumin, calbindin, or calretinin. Neuroscience 97, 47–58.

Bracci, E., Vreugdenhil, M., Hack, S.P., Jefferys, J.G., 1999. On the synchronizing mechanisms of tetanically induced hippocampal oscillations. J. Neurosci. 19, 8104–8113.

Bush, P.C., Prince, D.A., Miller, K.D., 1999. Increased pyramidal excitability and NMDA conductance can explain posttraumatic epileptogenesis without disinhibition: a model. J. Neurophysiol. 82, 1748–1758.

Caillard, O., Moreno, H., Schwaller, B., Llano, I., Celio, M.R., Marty, A., 2000. Role of the calcium-binding protein parvalbumin in short-term synaptic plasticity. Proc. Natl. Acad. Sci. U. S. A. 97, 13372–13377.

Cauli, B., Audinat, E., Lambolez, B., Angulo, M.C., Ropert, N., Tsuzuki, K., Hestrin, S., Rossier, J., 1997. Molecular and physiological diversity of cortical nonpyramidal cells. J. Neurosci. 17, 3894–3906.

Celio, M.R., Blümcke, I., 1994. Perineuronal nets—A specialized form of extracellular matrix in the adult nervous system. Brain Res. Rev. 19, 128–145.

Celio, M.R., Heizmann, C.W., 1982. Calcium-binding protein parvalbumin is associated with fast contracting muscle fibres. Nature 297, 504–506.

Celio, M.R., Spreafico, R., De Biasi, S., Vitellaro-Zuccarello, L., 1998. Perineuronal nets: past and present. Trends Neurosci. 21, 510–515.

Chagnac-Amitai, Y., Connors, B.W., 1989. Synchronized excitation and inhibition driven by intrinsically bursting neurons in neocortex. J. Neurophysiol. 62, 1149–1162.

Cohen, I., Navarro, V., Clemenceau, S., Baulac, M., Miles, R., 2002. On the origin of interictal activity in human temporal lobe epilepsy in vitro. Science 298, 1418–1421.

Congar, P., Leinekugel, X., Ben-Ari, Y., Crepel, V., 1997. A long-lasting calcium-activated nonselective cationic current is generated by synaptic stimulation or exogenous activation of group I metabotropic glutamate receptors in CA1 pyramidal neurons. J. Neurosci. 17, 5366–5379.

Cossart, R., Dinocourt, C., Hirsch, J.C., Merchan-Perez, A., De Felipe, J., Ben-Ari, Y., Esclapez, M., Bernard, C., 2001. Dendritic but not somatic GABAergic inhibition is decreased in experimental epilepsy. Nat. Neurosci. 4, 52–62.

Davies, C.H., Collingridge, G.L., 1993. The physiological regulation of synaptic inhibition by GABAB autoreceptors in rat hippocampus. J. Physiol. (London) 472, 245–265.

DeFelipe, J., 1997. Types of neurons, synaptic connections and chemical characteristics of cells immunoreactive for calbindin-D28K, parvalbumin and calretinin in the neocortex. J. Chem. Neuroanat. 14, 1–19.

DeFelipe, J., 1999. Chandelier cells and epilepsy. Brain 122, 1807–1822.

DeFelipe, J., Hendry, S.H., Jones, E.G., 1989. Visualization of chandelier cell axons by parvalbumin immunoreactivity in monkey cerebral cortex. Proc. Natl. Acad. Sci. U. S. A. 86, 2093–2097.

DeFelipe, J., Garcia Sola, R., Marco, P., del Rio, M.R., Pulido, P., Ramon y Cajal, S., 1993. Selective changes in the microorganization of the human epileptogenic neocortex revealed by parvalbumin immunoreactivity. Cereb. Cortex 3, 39–48.

Deisz, R.A., 2002. Cellular mechanisms of pharmacoresistance in slices from epilepsy surgery. Novartis Found. Symp. 243, 186–199.

Diesmann, M., Gewaltig, M.O., Aertsen, A., 1999. Stable propagation of synchronous spiking in cortical neural networks. Nature 402, 529–533.

Di Garbo, A., Barbi, M., Chillemi, S., 2002. Synchronization in a network of fast-spiking interneurons. BioSystems 67, 45–53.

Eisen, M.B., Brown, P.O., 1999. DNA arrays for analysis of gene expression. Methods Enzymol. 303, 179–205.

Engel Jr., J., 1996. Excitation and inhibition in epilepsy. Can. J. Neurol. Sci. 23, 167–174.

Ferraro, T.N., Golden, G.T., Smith, G.G., St Jean, P., Schork, N.J., Mulholland, N., Ballas, C., Schill, J., Buono, R.J., Berrettini, W.H., 1999. Mapping loci for pentylenetetrazol-induced seizure susceptibility in mice. J. Neurosci. 19, 6733–6739.

Fujiwara-Tsukamoto, Y., Isomura, Y., Nambu, A., Takada, M., 2003. Excitatory GABA input directly drives seizure-like rhythmic synchronization in mature hippocampal CA1 pyramidal cells. Neuroscience 119, 265–275.

Fukuda, T., Kosaka, T., 2000. Gap junctions linking the dendritic network of GABAergic interneurons in the hippocampus. J. Neurosci. 20, 1519–1528.

Gerlai, R., 1996. Gene-targeting studies of mammalian behavior: is it the mutation or the background genotype. Trends Neurosci. 19, 177–181.

Golfier, G., Tran Dang, M., Dauphinot, L., Graison, E., Rossier, J., Potier, M.-C., 2004. VARAN: a web server for VARiability ANalysis of DNA microarray experiments. Bioinformatics, in press.

Hajos, N., Papp, E.C., Acsady, L., Levey, A.I., Freund, T.F., 1998. Distinct interneuron types express m2 muscarinic receptor immunoreactivity on their dendrites or axon terminals in the hippocampus. Neuroscience 82, 355–376.

Hartley, D.M., Neve, R.L., Bryan, J., Ullrey, D.B., Bak, S.Y., Lang, P., Geller, A.I., 1996. Expression of the calcium-binding protein, parvalbumin, in cultured cortical neurons using a HSV-1 vector system enhances NMDA neurotoxicity. Mol. Brain Res. 40, 285–296.

Haunso, A., Ibrahim, M., Bartsch, U., Letiembre, M., Celio, M.R., Menoud, P., 2000. Morphology of perineuronal nets in tenascin-R and parvalbumin single and double knockout mice. Brain Res. 864, 142–145.

Hefti, B.J., Smith, P.H., 2000. Anatomy, physiology, and synaptic responses of rat layer V auditory cortical cells and effects of intracellular GABA(A) blockade. J. Neurophysiol. 83, 2626–2638.

Hendrickson, A.E., Van Brederode, J.F., Mulligan, K.A., Celio, M.R., 1991. Development of the calcium-binding protein parvalbumin and calbindin in monkey striate cortex. J. Comp. Neurol. 307, 626–646.

Hendry, S.H., Jones, E.G., Emson, P.C., Lawson, D.E., Heizmann, C.W., Streit, P., 1989. Two classes of cortical GABA neurons defined by differential calcium binding protein immunoreactivities. Exp. Brain Res. 76, 467–472.

Herrero, A.I., Del Olmo, N., Gonzalez-Escalada, J.R., Solis, J.M., 2002. Two new actions of topiramate: inhibition of depolarizing GABA(A)-mediated responses and activation of a potassium conductance. Neuropharmacology 42, 210–220.

Hof, P.R., Glezer I.I., Conde, F., Flagg, R.A., Rubin, M.B., Nimchinsky, E.A., Vogt Weisenhorn, D.M., 1999. Cellular distribution of the calcium-binding proteins parvalbumin, calbindin, and calretinin in the neocortex of mammals: phylogenetic and developmental patterns. J. Chem. Neuroanat. 16, 77–116.

Hooper, M., Hardy, K., Handyside, A., Hunter, S., Monk, M., 1987. HPRT-deficient (Lesh–Nyhan) mouse embryos derived from germline colonization by cultured cells. Nature 326, 292–295.

Jones, E.G., 1993. GABAergic neurons and their role in cortical plasticity in primates. Cereb. Cortex 3, 361–372.

Kaila, K., 1994. Ionic basis of GABAA receptor channel function in the nervous system. Prog. Neurobiol. 42, 489–537.

Kaila, K., Lamsa, K., Smirnov, S., Taira, T., Voipio, J., 1997. Long-lasting GABA-mediated depolarization evoked by high-frequency stimulation

in pyramidal neurons of rat hippocampal slice is attributable to a network-driven, bicarbonate-dependent K^+ transient. J. Neurosci. 17, 7662–7672.

Kawaguchi, Y., Kubota, Y., 1993. Correlation of physiological subgroupings of nonpyramidal cells with parvalbumin- and calbindinD28k-immunorective neurons in layer V of rat frontal cortex. J. Neurophysiol. 70, 387–396.

Kawaguchi, Y., Kubota, Y., 1997. GABAergic cell subtypes and their synaptic connections in rat frontal cortex. Cereb. Cortex 7, 476–486.

Kisvarday, Z.F., Kim, D.S., Eysel, U.T., Bonhoeffer, T., 1994. Relationship between lateral inhibitory connections and the topography of the orientation map in cat visual cortex. Eur. J. Neurosci. 6, 1619–1632.

Klapstein, G.J., Vietla, S., Lieberman, D.N., Gray, P.A., Airaksinen, M.S., Thoenen, H., Meyer, M., Mody, I., 1998. Calbindin-D28k fails to protect hippocampal neurons against ischemia in spite of its cytoplasmic calcium buffering properties: evidence from calbindin-D28k knockout mice. Neuroscience 85, 361–373.

Kohling, R., Vreugdenhil, M., Bracci, E., Jefferys, J.G., 2000. Ictal epileptiform activity is facilitated by hippocampal GABAA receptor-mediated oscillations. J. Neurosci. 20, 6820–6829.

Kosaka, T., Heizmann, C.W., 1989. Selective staining of a population of parvalbumin-containing GABAergic neurons in the rat cerebral cortex by lectins with specific affinity for terminal *N*-acetylgalactosamine. Brain Res. 483, 158–163.

Lambert, N.A., Wilson, W.A., 1994. Temporally distinct mechanisms of use-dependent depression at inhibitory synapses in the rat hippocampus in vitro. J. Neurophysiol. 72, 121–130.

Lambert, N.A., Harrison, N.L., Teyler, T.J., 1991. Evidence for mu opiate receptors on inhibitory terminals in area CA1 of rat hippocampus. Neurosci. Lett. 124, 101–104.

Lee, S.H., Rosenmund, C., Schwaller, B., Neher, E., 2000a. Differences in Ca^{2+} buffering properties between excitatory and inhibitory hippocampal neurons from the rat. J. Physiol. (London) 525, 405–418.

Lee, S.H., Schwaller, B., Neher, E., 2000b. Kinetics of Ca^{2+} binding to parvalbumin in bovine chromaffin cells: implications for $[Ca^{2+}]$ transients of neuronal dendrites. J. Physiol. (London) 525, 419–432.

Lewis, D.A., Lund, J.S., 1990. Heterogeneity of chandelier neurons in monkey neocortex: corticotropin-releasing factor- and parvalbumin-immunoreactive populations. J. Comp. Neurol. 293, 599–615.

Li, L., Kelly, J.B., 1992. Binaural responses in rat inferior colliculus following kainic acid lesions of the superior olive: interaural intensity difference functions. Hear. Res. 61, 73–85.

Lopantsev, V., Avoli, M., 1998. Participation of GABAA-mediated inhibition in ictallike discharges in the rat entorhinal cortex. J. Neurophysiol. 79, 352–360.

Loscher, W., Nolting, B., 1991. The role of technical, biological and pharmacological factors in the laboratory evaluation of anticonvulsant drugs: IV. Protective indices. Epilepsy Res. 9, 1–10.

Lüth, H.-J., Fischer, J., Celio, M.R., 1992. Soybean lectin binding neurons in the visual cortex of the rat contain parvalbumin and are covered by glial nets. J. Neurocytol. 21, 211–221.

Lytton, W.W., Sejnowski, T.J., 1991. Simulations of cortical pyramidal neurons synchronized by inhibitory interneurons. J. Neurophysiol. 66, 1059–1079.

Marco, P., Sola, R.G., Pulido, P., Alijarde, M.T., Sanchez, A., Cajal, S.R.Y., DeFelipe, J., 1996. Inhibitory neurons in the human epileptogenic temporal neocortex—An immunocytochemical study. Brain 119, 1327–1347.

Meier, T.J., Ho, D.Y., Sapolsky, R.M., 1997. Increased expression of calbindin D-28k via herpes simplex virus amplicon vector decreases calcium ion mobilization and enhances neuronal survival after hypoglycemic challenge. J. Neurochem. 69, 1039–1047.

Mihaly, A., Szente, M., Dubravcsik, Z., Boda, B., Kiraly, E., Nagy, T., Domonkos, A., 1997. Parvalbumin- and calbindin-containing neurons express c-fos protein in primary and secondary (mirror) epileptic foci of the rat neocortex. Brain Res. 761, 135–145.

Mohler, H., Benke, D., Benson, J., Luscher, B., Fritschy, J.M., 1995. GABAA-receptor subtypes in vivo: cellular localization, pharmacology and regulation. Adv. Biochem. Psychopharmacol. 48, 41–56.

Oka, J.I., Kobayashi, T., Nagao, T., Hicks, T.P., Fukuda, H., 1993. GABAA receptor-induced inhibition of neuronal burst firing is weak in rat somatosensory cortex. NeuroReport 4, 731–744.

Olsen, R.W., 1981. The GABA postsynaptic membrane receptor–ionophore complex. Site of action of convulsant and anticonvulsant drugs. Mol. Cell. Biochem. 39, 261–279.

Otis, T.S., De Koninck, Y., Mody, I., 1994. Lasting potentiation of inhibition is associated with an increased number of gamma-aminobutyric acid type A receptors activated during miniature inhibitory postsynaptic currents. Proc. Natl. Acad. Sci. U. S. A. 91, 7698–7702.

Perkel, D.H., Gerstein, G.L., Moore, G.P., 1967a. Neuronal spike trains and stochastic point processes: I. The single spike train. Biophys. J. 7, 391–418.

Perkel, D.H., Gerstein, G.L., Moore, G.P., 1967b. Neuronal spike trains and stochastic point processes: II. Simultaneous spike trains. Biophys. J. 7, 419–440.

Plogmann, D., Celio, M.R., 1993. Intracellular concentration of parvalbumin in nerve cells. Brain Res. 600, 273–279.

Potier, M.-C., Gibelin, N., Cauli, B., Le Bourdelles, B., Lambolez, B., Golfier, G., Kuhlmann, S., Marc, P., Devaux, F., Rossier, J., 2002. Development of microarrays to study gene expression in tissue and single cells: analysis of neural transmission. Microarrays for the Neurosciences: An Essential Guide. MIT Press, Cambridge, MA, pp. 237–254.

Prince, D.A., 1999. Epileptogenic neurons and circuits. Adv. Neurol. 79, 665–684.

Prince, D.A., Jacobs, K., 1998. Inhibitory function in two models of chronic epileptogenesis. Epilepsy Res. 32, 83–92.

Prince, D.A., Jacobs, K.M., Salin, P.A., Hoffman, S., Parada, I., 1997. Chronic focal neocortical epileptogenesis: does disinhibition play a role? Can. J. Physiol. Pharmacol. 75, 500–507.

Schena, M., Shalon, D., Davis, R.W., Brown, P.O., 1995. Quantitative monitoring of gene expression patterns with a complementary DNA microarray. Science 270, 467–470.

Schierle, G.S., Gander, J.C., Dorlando, C., Celio, M.R., Weisenhorn, D.M.V., 1997. Calretinin-immunoreactivity during postnatal development of the rat isocortex: a qualitative and quantitative study. Cereb. Cortex 7, 130–142.

Schiffmann, S.N., Cheron, G., Lohof, A., d'Alcantara, P., Meyer, M., Parmentier, M., Schurmans, S., 1999. Impaired motor coordination and Purkinje cell excitability in mice lacking calretinin. Proc. Natl. Acad. Sci. U. S. A. 96, 5257–5262.

Schwaller, B., Buchwald, P., Blumcke, I., Celio, M.R., Hunziker, W., 1993. Characterization of a polyclonal antiserum against the purified human recombinant calcium binding protein calretinin. Cell Calcium 14, 639–648.

Schwaller, B., Dick, J., Dhoot, G., Carroll, S., Vrbova, G., Nicotera, P., Pette, D., Wyss, A., Bluethmann, H., Hunziker, W., 1999. Prolonged contraction–relaxation cycle of fast-twitch muscles in parvalbumin knockout mice. Am. J. Physiol. 276, C395–C403.

Schwaller, B., Meyer, M., Schiffmann, S.N., 2002. "New" functions for "old" proteins: the role of the calcium-binding proteins calbindin D-28k, calretinin and parvalbumin, in cerebellar physiology. Studies with knockout mice. Cerebellum 1, 241–258.

Scotti, A.L., Kalt, G., Bollag, O., Nitsch, C., 1997. Parvalbumin disappears from GABAergic CA1 neurons of the gerbil hippocampus with seizure onset while its presence persists in the perforant path. Brain Res. 760, 109–117.

Solbach, S., Celio, M.R., 1991. Ontogeny of the calcium binding protein parvalbumin in the rat nervous system. Anat. Embryol. 184, 103–124.

Somogyi, P., Tamas, G., Lujan, R., Buhl, E.H., 1998. Salient features of synaptic organisation in the cerebral cortex. Brain Res. Brain Res. Rev. 26, 113–135.

Soriano, E., Del Rio, J.A., Ferrer, I., Auladell, C., De Lecea, L., Alcantara, S., 1992. Late appearance of parvalbumin-immunoreactive neurons in the rodent cerebral cortex does not follow an 'inside–out' sequence. Neurosci. Lett. 142, 147–150.

Stone, W.E., Javid, M.J., 1979. Quantitative evaluation of the actions of anticonvulsants against different chemical convulsants. Arch. Int. Pharmacodyn. Ther. 240, 66–78.

Thomson, A.M., 1997. Activity-dependent properties of synaptic transmission at two classes of connections made by rat neocortical pyramidal axons in vitro. J. Physiol. (London) 502, 131–147.

Traub, R.D., Borck, C., Colling, S.B., Jefferys, J.G., 1996. On the structure of ictal events in vitro. Epilepsia 37, 879–891.

Veliskova, J., Velisek, L., Moshe, S.L., 1996. Age-specific effects of baclofen on pentylenetetrazol-induced seizures in developing rats. Epilepsia 37, 718–722.

Villa, A.E., 1990. Physiological differentiation within the auditory part of the thalamic reticular nucleus of the cat. Brain Res. Brain Res. Rev. 15, 25–40.

Villa, A.E., Tetko, I.V., Hyland, B., Najem, A., 1999. Spatiotemporal activity patterns of rat cortical neurons predict responses in a conditioned task. Proc. Natl. Acad. Sci. U. S. A. 96, 1106–1111.

Villa, A.E.P., Dutoit, P., Tetko, I.V., Hunziker, W., Celio, M., Schwaller, B., 2000. Non-linear coupling of local field potentials across cortical sites in parvalbumin-deficient mice. In: Lehnertz, K., Arnhold, J., Grassberger, P., Elger, C.E. (Eds.), Chaos in Brain? World Scientific Publishing Co. Pte. Ltd., Singapore, pp. 243–246.

Vreugdenhil, M., Jefferys, J.G.R., Celio, M.R., Schwaller, B., 2003. Parvalbumin-deficiency facilitates repetitive IPSCs and related inhibition-based gamma oscillations in the hippocampus. J. Neurophysiol. 89, 1414–1423.

Whittington, M.A., Traub, R.D., Jefferys, J.G., 1995. Erosion of inhibition contributes to the progression of low magnesium bursts in rat hippocampal slices. J. Physiol. (London) 486, 723–734.

Yonekawa, W.D., Kupferberg, H.J., Woodbury, D.M., 1980. Relationship between pentylenetetrazol-induced seizures and brain pentylenetetrazol levels in mice. J. Pharmacol. Exp. Ther. 214, 589–593.

Zimmer, A., 1996. Gene targeting and behaviour: a genetic problem requires a genetic solution. Trends Neurosci. 19, 470.